Automated recognition of the psoas major muscles on X-ray CT images

N. Kamiya, X. Zhou, H. Chen, T. Hara, H. Hoshi, R. Yokoyama, M. Kanematsu, and H. Fujita

Abstract—The purpose of this study is to recognize the psoas major muscle on X-ray CT images. For this purpose, we propose a novel recognition method. The recognition process in this method involves three steps: the generation of a shape model for the psoas major muscle, recognition of anatomical points such as the origin and insertion, and the recognition of the psoas major muscles by the use of the shape model. We generated the shape model using 20 CT cases and tested the model for recognition in 20 other CT cases. The average Jaccard similarity coefficient (JSC) and reproducibility rate were 0.704 and 0.783, respectively. Experimental results indicate that our method was effective for a 2-D cross-sectional area (CSA) analysis.

I. INTRODUCTION

IN aging societies, it is very important to analyze age-related hypokinesia. In Japan, elderly people being physically handicapped after suffering a fall is becoming a social issue. Sixty-two percent of the falls result in physical damage, of which 12% result in bone fractures and 8% result in the victims "requiring constant help and care" [1]. Therefore, maintaining the quality of life (QOL) of the elderly is a critical task in the field of healthcare for the aged [2]. In addition, the abovementioned statistics correspond to events that occur inside the house; elderly people fall during routine everyday movements. Thus, proactive measures are required to protect the elderly. Factors affecting the falls suffered by elderly people include sensory lineage, the state of the ocular system, skeletal musculature, balancing mechanisms, higher nervous activity, heavy medication, and changes in sleep patterns. Here, we focus on skeletal musculature, which decreases with age.

It is considered that elderly people fall because of weakness in the muscles at the lower extremities. Atrophy of the psoas major muscles affects the ability of elderly people to walk and exercise [3]. In addition, it is difficult for female

N. Kamiya is with the Department of Intelligent Image Information, Division of Regeneration and Advanced Medical Sciences, Graduate School of Medicine, Gifu University, Yanagido 1-1, Gifu 501-1194, Japan (phone: +81(58)-230-6515; fax: +81(58)-230-6514; e-mail: kamiya@fjt.info.gifu-u.ac.jp).

X. Zhou, T. Hara, and H. Fujita are with the Department of Intelligent Image Information, Division of Regeneration and Advanced Medical Sciences, Graduate School of Medicine, Gifu University, Yanagido 1-1, Gifu 501-1194, Japan.

H. Chen is with the Department of Anatomy, Graduate School of Medicine, Gifu University, Gifu 501-1194, Japan.

R. Yokoyama and M. Kanematsu are with the Department of Radiology Services, Gifu University Hospital, Gifu 501-1194, Japan.

M. Kanematsu is with the Department of Radiology, Gifu University School of Medicine and Gifu University Hospital, Gifu 501-1194, Japan.

H. Hoshi is with the Department of Radiology, Division of Tumor Control, Graduate School of Medicine, Gifu University, Gifu 501-1194, Japan.

patients to maintain the condition of these muscles, which is measured in terms of the cross-sectional area (CSA), solely by daily exercise; furthermore, the CSA decreases more rapidly with age. Therefore, because the decrease in the CSA of the psoas major muscles is higher for septuagenarians and the elderly than for any other age group, it is necessary to protect the psoas major muscles from age-related damage [3].

We developed a computer-aided diagnosis (CAD) system for diagnosing the torso region using non-contrast CT images in which the skeletal muscles are in focus [4, 5]. Our aim is to measure the skeletal muscles automatically. Currently, a CAD system is required for clinical situations. Recently, we have been able to rapidly obtain high-definition CT images; however, the number of images increases to as many as a thousand slices per patient, causing radiologists to neglect the areas in the displayed images that are of no interest when targeting specific diseases. Therefore, we have developed the CAD system as an aid for radiologists.

In this paper, we propose a novel method to automatically recognize the psoas major muscles in non-contrast X-ray CT images of the torso. The key steps that this method is based on are the generation of a shape model for the psoas major muscles and the application of a recognition process. In this process, we automatically obtain pathognomonical points as landmarks (LM) on the basis of anatomical positional information on the region between the muscle and skeleton. Then, we use the proposed method of creating an anatomical centerline for the muscle in order to describe the muscle fiber directions. Next, we extract the regions that show the muscles. At this point, the psoas major muscles are deep muscles, and hence, we utilize the anatomical centerline to create the shape model. Then, we recognize the muscles using density information for the regions generated by the use of the model. Finally, we estimate the CSA and compare the manually obtained results with those obtained using this method. The results indicate the effectiveness of applying the principles behind this method.

II. METHODS

The psoas major muscles cover the anterolateral surface of the bodies of the lumbar vertebrae and fill the space between the vertebral bodies and transverse processes. Each of these muscles originates from the bodies of vertebra XII and other four lumbar vertebras. These muscles pass inferiorly along the pelvic brim and attach to the lesser trochanter of the femur; the point of attachment is the insertion [6]. We treat the origin and insertion as LMs. Then, the corresponding LMs are connected by a straight line called the anatomical centerline, which represents the direction of the muscle fiber. We create five anatomical centerlines between the corresponding LMs. Further, the muscle is found to be the thickest in the center, and it connects the origin and insertion.

TABLE I
CORRESPONDENCE BETWEEN THE ORIGIN AND INSERTION

Origin	Insertion
Thoracic vertebra XII	
Lumbar vertebra I	Barycenter of
Lumbar vertebra II	lacuna
Lumbar vertebra III	musculorum
Lumbar vertebra IV	

We approximate its shape by using the quadratic function included in the shape model of the psoas major muscles. In the recognition process, we automatically recognize LMs to create the anatomical centerline and utilize the shape model for the psoas major muscles.

A. Shape Model Generation

The first author manually extracted the regions showing the psoas major muscle, and the results were inspected and revised by the third author, who is an expert on anatomy. In this study, we used 20 CT cases in which no lesions or atrophying occurred within the target region. Next, we manually input pathognomonic points. Table I shows the origin and insertion of the psoas major muscles. In this table, the insertion was anatomically defined by the lesser trochanter of the femur; however, this model was generated by using the barycenter of the lacuna musculorum instead because the CT image of the torso does not always include the lesser trochanter of the femur. In addition, in this method, the origin and insertion were used for determining an anatomical centerline so that they were aligned. Next, the Euclidian distance technique was applied to this manually extracted region to obtain a distance value from the anatomical centerlines (Fig. 1). This value represents the distance between the centerline and the border of the psoas major muscles.

In this method, this distance value was normalized by the distance from the midpoint, which was measured from the midpoint of the anatomical centerline. These normalized values were included in the database used in the study. Then, we approximated the quadratic curve by using the value for each anatomical centerline. Figure 2 shows the obtained patterns. We approximated the quadratic curve $y_i = \alpha_i x_i^2 + \beta_i$. In this function, α_i is the gradient represented by the shape of the outer psoas major muscles; β_i is the maximum value of the function and indicates the intercept of the function since it yields the approximate value of the greatest dimension of this muscle (i.e., the maximum value of the function is attained at the midpoint between the origin and insertion); x_i is used in the recognition process to calculate y_i by substitution.

Table II lists the outer shape model generated by a quadratic curve approximation. The α_i for each origin was determined as -1.81×10^{-4}, -4.29×10^{-4}, -5.68×10^{-4}, -8.01×10^{-4}, and -9.20×10^{-4}, respectively. β_i is determined in the subsequent recognition process rather than in this process.
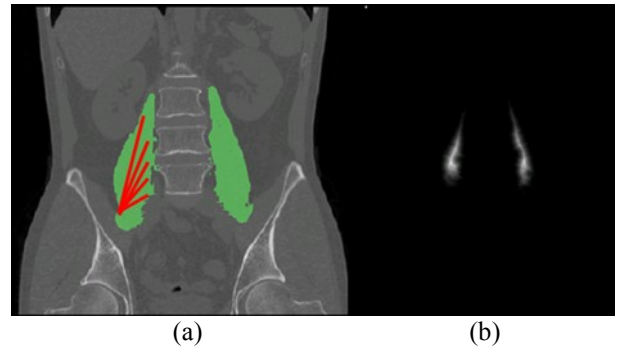

(a)   (b)

Fig. 1. Diagrams for shape model generation. (a) Patterns showing five anatomical centerlines on the psoas major muscles identified manually. (b) Image showing Euclidian distance from centerline to the border.
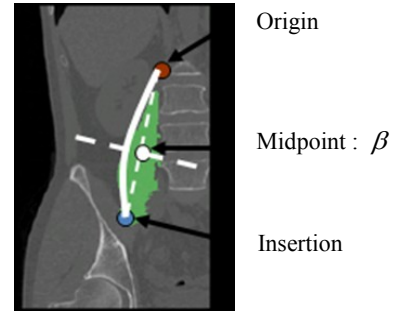

Fig. 2. Diagram for the shape model (solid line). The outer shape of the psoas major muscle is approximated using a quadratic curve.

TABLE II
SHAPE MODEL FUNCTION

Origin	Approximate functions	R^2 value
Thoracic vertebra XII	$y_1 = -1.81 \times 10^{-4} x_1^2 + \beta_1$	0.753
Lumbar vertebra I	$y_2 = -4.29 \times 10^{-4} x_2^2 + \beta_2$	0.902
Lumbar vertebra II	$y_3 = -5.68 \times 10^{-4} x_3^2 + \beta_3$	0.855
Lumbar vertebra III	$y_4 = -8.01 \times 10^{-4} x_4^2 + \beta_4$	0.765
Lumbar vertebra IV	$y_5 = -9.20 \times 10^{-4} x_5^2 + \beta_5$	0.660

This table indicates that the average R^2 value is 0.787, the maximum value is 0.902, and the minimum value is 0.660. In particular, we obtained a relatively low R^2 value for L4.

B. Anatomical Feature Point Recognition

Before the recognition process, we must automatically recognize the pathognomonical points as LMs. In this section, we explain the automatic LM recognition method. Each LM is detected automatically on the basis of the anatomical origin and insertion. The location of the LM on the segmented skeletal image [4] was determined by its spatial anatomical position information. Table I lists the anatomical origins and insertions that are used in this method as LMs in the same manner as in the manual extraction process discussed in section A.

To determine the location of each origin, we use positional information for each skeleton from Th12 to L4. First, we determine the z coordinate of the body axis by determining the barycenter of each skeleton (Fig. 3(a)). Next, we determine the x and y coordinates. This is a bilaterally symmetric process. Then, the median point on the axial plane
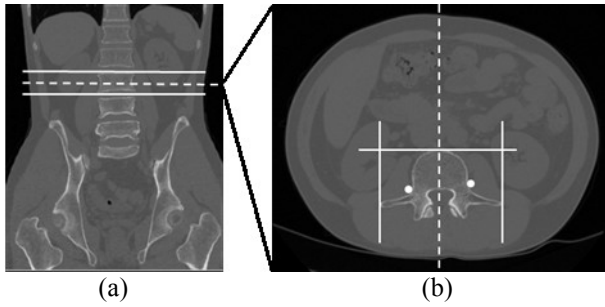
Fig. 3. Diagram showing anatomical feature point recognition. (a) Slice decision (dotted line) using position information for the upper and lower skeleton. (b) Anatomical feature point recognition; the dashed line shows the line of symmetry, the solid line shows the area that was searched, and white circle shows a recognized point.
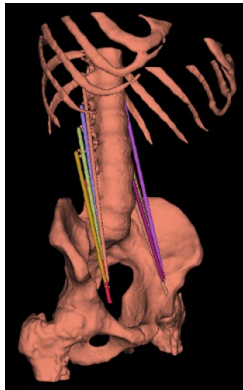

Fig. 4. 3-D image of a skeleton with anatomical centerlines. Each color represents a different anatomical centerline.

within the region including the human body region was calculated; the symmetry line is shown by the dashed line in Fig. 3(b). Therefore, on the basis of the area enclosed by the solid line in Fig. 3(b), we recognize the white circle automatically.

In determining the insertion, we use the barycenter of lacuna musculorum, as indicated above. The lacuna musculorum was automatically recognized by using our previous method [7]. In this study, we calculate the barycenter of this area to be an insertion LM.

Finally, we use these LMs to generate an anatomical centerline. In this study, we connect each origin and insertion by a straight line. Figure 4 shows a 3-D image of a skeleton with an anatomical centerline. Each generated line is symmetric with respect to the vertebral column.

C. Recognition Process

We utilize this shape model to recognize the psoas major muscles in unknown test cases. As a preliminary step, we recognize anatomical points and generate an anatomical centerline.

First, we complete the development of the shape model and determine β_i for each anatomical centerline. Here, the distance from the midpoint to the origin or insertion was substituted for x_i, and then the muscle diameter, which is zero at this point, was substituted for y_i. After this calculation,
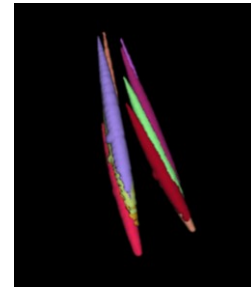

Fig. 5. Mask image generated by shape model function. Each color represents the mask of each anatomical centerline.
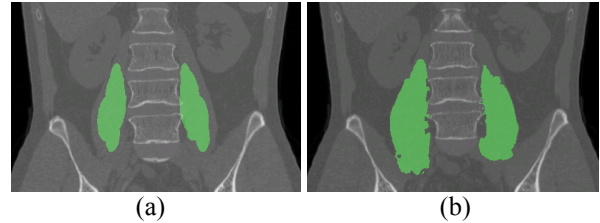

Fig. 6. Recognition results superimposed over the original CT image. The green region represents the recognition results obtained using the proposed method. (a) Initial results; (b) results obtained using the extraction method after initial recognition.

we use this function to recognize the psoas major muscles. Then, we search the muscle region within the created sphere to substitute the distance of the midpoint to centerline for x_i. Figure 5 shows the mask image. After this process, we create a short list of regions that possibly show skeletal muscles by using the Otsu method [8] in order to set an initial region (Fig. 6(a)). In addition, there are cases in which the model function recognizes an area smaller than the real region. In these CT cases, we recognize the surrounding region by using a radial pattern up to the boundary. However, if the boundary was not detected and the radius was larger than it at the midpoint of the centerline, the implementation of this dilation method is halted as the boundary would connect to other tissues. Figure 6(b) shows the recognition results after the extraction method has been implemented.

III. RESULTS AND DISCUSSION

We adopted this scheme in 20 CT cases with non-contrast torso X-ray CT images and evaluated the accuracy of the recognition results; the evaluation was based on the overlap rate between the recognized and manually extracted regions that were created by an author under the guidance of the anatomical specialist. The Jaccard similarity coefficient (JSC) [9] and reproducibility rates were used to evaluate the effectiveness of the proposed methods. The former is calculated by $\frac{A \cap B}{A \cup B}$ and the latter by $\frac{A \cap B}{A}$. A and B represent the regions corresponding to the gold standard and recognition results, respectively. The JSC rates are calculated in the 3-D volume as well as the CSA for each of the vertebral bodies.

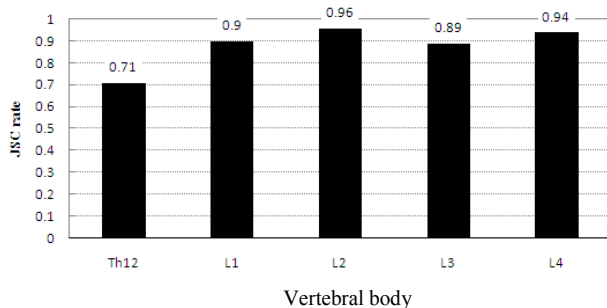|	JSC rate	Reproducibility rate
Min.	0.641	0.677
Max.	0.894	0.984
Ave.	0.704	0.783

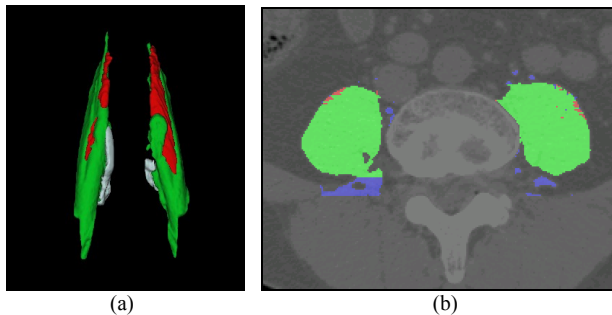Fig. 7. Average JSC rate of the CSA in each vertebral body for 20 cases.

(a)   (b)

Fig. 8. Recognition results with gold standard. (a) 3-D view of the recognition results. (b) Example of the recognition results for the CSA. Green represents the area of overlap, blue represents the area of overextraction, and red represents the area of underextraction.
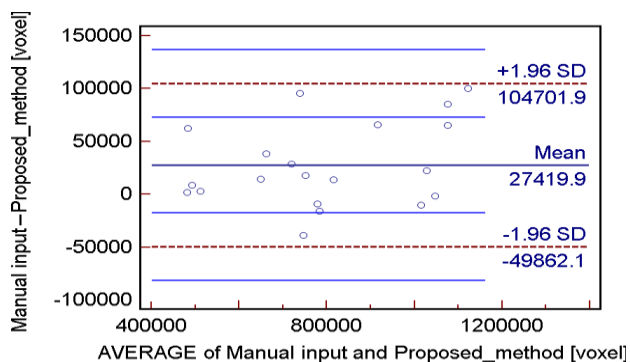

Fig. 9. Bland & Altman plot showing a scatter diagram of the differences plotted against the averages of the two measurements.

Table III lists the values of the recognition results. The average value is approximately 0.7–0.8%. This figure is not sufficiently high for measuring the muscle volume. Figure 7 shows the JSC rate of the CSA in each vertebral body. In this figure, the high JSC rate is observed at the cross-sections of L1 to L4. Figure 8 shows the recognition results. Figure 8(a) shows the 3-D view; the green region is the area of overlap between the gold standard and recognition results, the blue area is the area of overextraction, and the red area is the area of underextraction. Figures 7 and 8(a) indicate that our

method needs improvement for the upper region. However, the JSC rates for the middle and lower regions were high. The JSC rate at the cross-section of L3 is lower than that at the cross-sections of L2 and L4 because of false recognition of the vessel; this case is shown by the blue region in Figure 8(a). In clinical practice, a radiologist measures the CSA or thickness at the cross-section called the Jacoby line. This line is located approximately at the cross-sections of L4 to L5, and one example is shown in Figure 8(b). In the 20 tested CT cases, the mean error in the thickness at the Jacoby line is 3 mm. This result shows that our method can be used to automatically and quantitatively measure the thickness of psoas major muscles. Figure 9 shows the Bland & Altman plot for the manually extracted regions and the regions obtained by using our proposed method. This result confirms that the two methods may be used interchangeably, because all the differences lie within the mean $\pm$ 1.96 SD.

IV. CONCLUSION

We proposed a fully automated method to recognize psoas major muscles in X-ray CT images of the torso. This method was utilized in 40 CT cases. The average values for the JSC and reproducibility rates were 0.704 and 0.783, respectively. These results agree with the 2-D results obtained in clinical practice. We confirmed that our results comfortably satisfy the requirements for 2-D analysis in terms of the CSA and muscle thickness at the anatomical cross-section.

REFERENCES

[1] Cabinet Office, "Annual Report on the Aging Society: 2006," Available:http://www8.cao.go.jp/kourei/english/annualreport/2006/06 wp-e.html
[2] D. L. Sturnieks, R. St. George, S. R. Lord, "Balance disorders in the elderly," Neurophysiol Clin., vol. 38, no. 6, pp.467-78, 2008.
[3] K. Takahashi, H. E. Takahashi, H. Nakadaira, M. Yamamoto, "Different changes of quantity due to aging in the psoas major and quadriceps femoris muscles in women," J Musculoskelet Neuronal Interact., vol. 6, no. 2, pp. 201-5, 2006.
[4] X. Zhou, T. Hara, H. Fujita, R. Yokoyama, T. Kiryu, M. Kanematsu, and H. Hoshi, "Preliminary study for automated recognition of anatomical structure from torso CT images," in Proc. 27th. Annu. Conf. Eng. Medicine Biol. (EMBC), Shanghai, China, Sep. 2005, #340, in CD-ROM.
[5] X. Zhou, N. Kamiya, T. Hara, H. Fujita, H. Chen, R. Yokoyama, and H. Hoshi, "Automated segmentation and recognition of abdominal wall muscles in X-ray torso CT images and its application in abdominal CAD," International Journal of Computer Assisted Radiology and Surgery, vol. 2, Supplement. 1, pp. 389-90, 2007.
[6] R. Drake, W. Vogl, and A. W. M. Mitchell, "Gray's anatomy for students," Churchill Livingstone, 2005.
[7] S. Kojima, X. Zhou, T. Hara, H. Fujita, K. Azuma, R. Yokoyama, and H. Hoshi, "Automated analysis of bone structures for anatomical structure recognitions on torso X-ray CT images," IEICE technical report (in Japanese), vol. 106, no. 343, pp.43-8, 2006.
[8] N. Otsu, "A threshold selection method from gray-level histograms," IEEE Syst., Man, Cybern. C, vol. SMC-9, no. 1, pp. 62-66, 1979.
[9] M.R.Anderberg, Cluster Analysis for Applications, Academic Press, U.S.A., 1973.